Macromolecules

pubs.acs.org/Macromolecules Article

Copolymerization of Ethylene and Methyl Acrylate by Pyridylimino Ni(II) Catalysts Affording Hyperbranched Poly(ethylene-*co*-methyl acrylate)s with Tunable Structures of the Ester Groups

Zeinab Saki, Ilaria D'Auria, Anna Dall'Anese, Barbara Milani,* and Claudio Pellecchia*

Cite This: *Macromolecules* 2020, 53, 9294–9305 Read Online

ACCESS | Metrics & More | Article Recommendations | Supporting Information

ABSTRACT: The introduction of polar functional groups into the polyolefin skeleton is a challenging goal of high interest, and coordination-insertion polymerization represents the most powerful and environmentally friend approach to achieve it. Until now the most considerable catalysts are based on Pd(II) complexes and only a few examples on Ni(II) derivatives have been reported. We have now investigated a series of Ni(II) complexes with four pyridylimino ligands, both aldimines and ketimines, differing for the substituent present in position 6 on the pyridine ring (either a methyl group or a 2,6-dimethyl-substituted phenyl ring). These complexes generated active catalysts for the copolymerization of ethylene with methyl acrylate, yielding low-molecular weight, hyperbranched copolymers with the polar monomer content ranging between 0.2 and 35 mol % and inserted in a variety of modes, some of which were never observed before. The way of incorporation of the polar monomer goes from "*in-chain* only" to "everywhere but *in-chain*", and it is dictated by both the activation mode and the solvent used to dissolve the nickel precatalyst.

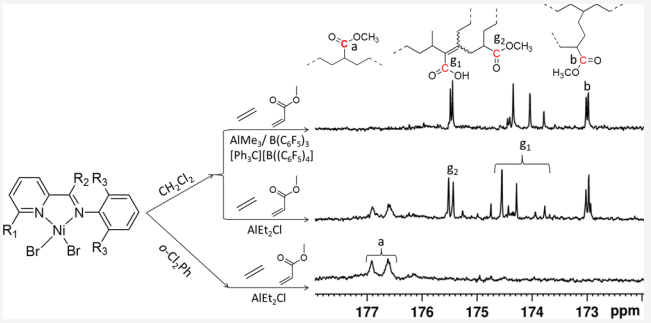

INTRODUCTION

Copolymers of ethylene with polar vinyl monomers, such as methyl acrylate or vinyl acetate, are commercially relevant products. The industrial production is currently based on radical processes, since the incorporation of vinyl polar monomers in olefin-based polymers via metal-catalyzed copolymerization remains challenging.[1] In fact, both traditional Ziegler-Natta and homogeneous metallocene/post-metallocene catalysts based on oxophilic Group 4 metals are easily deactivated by vinyl polar monomers lacking a spacer between the C=C double bond and the polar functionality.[1] Brookhart's α-diimine[2,3] and Drent's phosphine-sulfonate[4] Pd catalysts represented breakthrough advances in the field: the former produces highly branched copolymers of ethylene (E) with, e. g., methyl acrylate (MA), where the inserted MA units are localized at the end of the branches, while the latter provides access to linear E-MA copolymers with MA units inserted in the main chain. Following these initial discoveries, a large number of Pd complexes of the two classes displaying a variety of ligand modifications have been synthesized and tested.[5−7] In the α-diimine family, variations deal with the ligand skeleton,[8,9] desymmetrization,[10−13] and bulkiness.[14−16]

Recently, somewhat different ancillary ligand structures have been investigated for the development of Pd catalysts, including bisphosphine monoxide,[17] phosphine diethyl phosphonate,[18] phosphine phosphonic amide,[19] N-heterocyclic carbene-quinolinolate,[20] and phosphonic diamide phosphine,[21] resulting in some performance improvements.

Although a comparably large number of Ni(II) complexes in a variety of coordination environments has been investigated as precatalysts for the polymerization of ethylene,[22−24] examples of Ni catalysts active in the copolymerization with polar monomers are much scarcer. In several cases, their scope is limited to the copolymerization of some special polar monomers, e. g., the first salicylaldimine-nickel complex reported by Grubbs in 2000 was only able to copolymerize ethylene with substituted norbornenes (Chart 1, complex **A**).[25] Brookhart, Daugulis et al. recently reported that well-defined cationic [α-diimine-NiMe(L)]$^+$ catalysts (possibly generated in situ by activation of [α-diimine-$NiBr_2$] complexes with mixtures of $AlMe_3$ and B-based ionizing agents such as $B(C_6F_5)_3$ and $[Ph_3C][B(C_6F_5)_4]$) copolymerize ethylene with vinyltrialkoxysilanes but not with methyl acrylate (Chart 1, complex **B**).[26,27] Similar behaviors were observed by Chen using sterically encumbered Drent-type phosphine-sulfonate[28] or phosphine phosphonic amide[29] Ni catalysts and by Nozaki

Received: July 22, 2020
Revised: October 14, 2020
Published: October 28, 2020

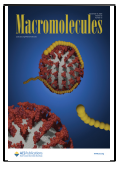

https://dx.doi.org/10.1021/acs.macromol.0c01703
Macromolecules 2020, 53, 9294–9305

Chart 1. Examples of Ni-Based Precatalysts for the Ethylene/Polar Vinyl Monomer Copolymerization (A-G) and Previously Reported 6-Aryl-Pyridylimino Complex H

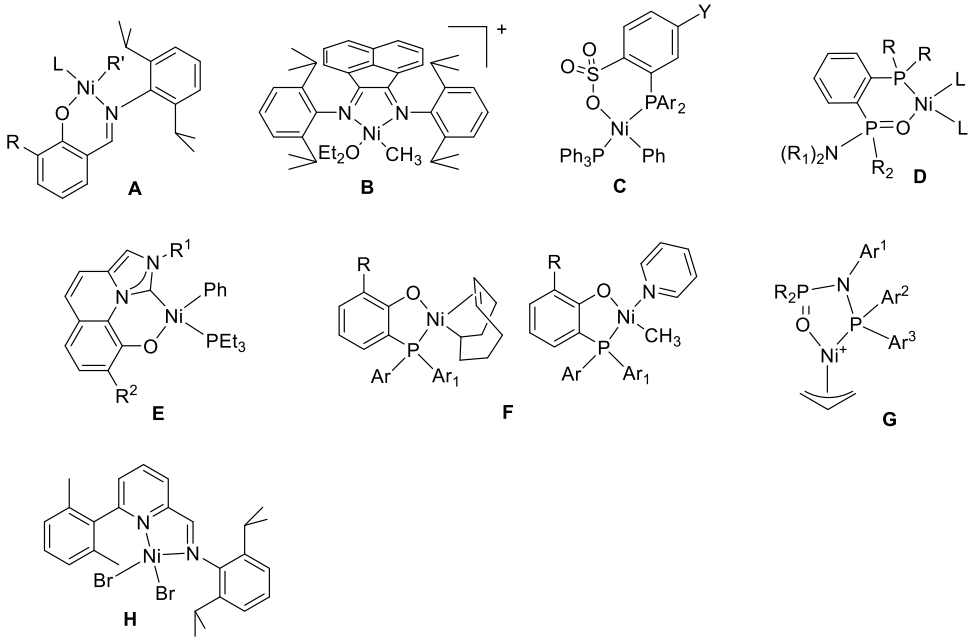

using N-heterocyclic carbene-quinolinolate Ni catalysts (Chart 1, complexes **C-E**).[30] Efficient copolymerization of ethylene with several vinyl polar monomers, including methyl acrylate, was instead achieved by Shimizu et al. using bis(aryl)-phosphinophenolate Ni(II) catalysts (Chart 1, complexes **F**).[31] Improved modified catalysts of the same class were then reported by Li et al.[32] Noteworthy are also the diphosphazane monoxide ligands developed by Chen, which peculiarly afford both Pd and Ni catalysts for ethylene-acrylate copolymerizations (Chart 1, complex **G**).[33]

Pyridylimino Ni(II) complexes have been widely investigated as catalysts for ethylene polymerization.[34−37] Most of the reported complexes display a variety of substitutents at the arylimino moiety, while only a few bear substituents on the pyridine ring. Different effects of the latter substitution have been reported, e.g., Laine et al. showed that introduction of a methyl in the position 6 of the pyridine ring resulted in a polyethylene with less branching and a slightly higher molecular weight;[34] Kempe et al. reported that introduction of bulky aryl substituents in the same position resulted in prevailingly ethylene dimerization;[36] and Antonov et al. found no direct correlation between the molecular weight and the nature of the pyridine substituent.[38] We have recently reported that the pyridylimino complex **H** (Chart 1) activated by $AlEt_2Cl$ affords hyperbranched low-molecular weight polyethylenes.[39] Experimental and theoretical evidences indicated that steric hindrance in the *ortho* position of the pyridine moiety destabilizes ethylene coordination, favoring both chain transfer and chain walking over propagation. We speculated that destabilization of ethylene coordination could reduce the reactivity gap of a monomer such as methyl acrylate. We have thus synthesized four related complexes bearing different substituents at the pyridino and at the imino moieties (complexes **Ni1−Ni4**, see Scheme 1) and tested them in the copolymerization of ethylene with methyl acrylate, resulting in the production of low-molecular weight hyperbranched poly(ethylene-*co*-methyl acrylate)s with MA

Scheme 1. Synthesis of the Ni Complexes Ni1−Ni4

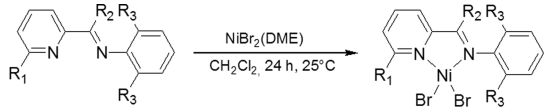

L^1: R_1 = 2,6-Me_2Ph, R_2 = Me, R_3 = *i*-Pr
L^2: R_1 = 2,6-Me_2Ph, R_2 = H, R_3 = Me
L^3: R_1 = Me, R_2 = H, R_3 = *i*-Pr
L^4: R_1 = Me, R_2 = Me, R_3 = *i*-Pr

Ni1 = L^1NiBr_2
Ni2 = L^2NiBr_2
Ni3 = L^3NiBr_2
Ni4 = L^4NiBr_2

molar contents ranging between 0.2 and 35%, and, intriguingly, with a variable mode of comonomer insertion, depending on the reaction conditions.

RESULTS AND DISCUSSION

The pyridylimino proligands were synthesized following previously reported procedures.[34,35,39] The nickel complexes **Ni1−Ni4** were obtained, in about 90% yields, by allowing the reaction of (dimethoxyethane)nickel dibromide and a slight excess of the proper ligand in methylene chloride, at 25 °C for 24 h (Scheme 1). The new complexes **Ni1** and **Ni2** were characterized by high resolution electrospray ionization Fourier transform ion cyclotron resonance (HR ESI FT-ICR) mass spectroscopy (see the Experimental Section and Figures S1 and S2; for the structurally closely related complex **H** a single crystal X-ray structure has been recently reported, confirming a monomeric Ni atom in a distorted tetrahedral coordination[39]). Complex **Ni3** and **Ni4** were reported previously.[34,40]

Complexes **Ni1−Ni4** were preliminarily tested in the homopolymerization of ethylene after activation with $AlEt_2Cl$ (200 equiv) at 40 °C and 6 atm monomer pressure: under these reaction conditions, all the complexes afforded hyperbranched low-molecular weight polyethylene oils, soluble in methanol, similar to those produced by complex **H**[39] (see the Supporting Information) and a few related Ni complexes.[41] Complexes **Ni1−Ni4** were then tested in the copolymerization of ethylene and methyl acrylate, after activation with 200

https://dx.doi.org/10.1021/acs.macromol.0c01703
Macromolecules 2020, 53, 9294−9305

Table 1. Ethylene-Methyl Acrylate Copolymerizations by Complexes Ni1−Ni4 under 6 atm of Ethylene[a]

run (sample)	Ni catalyst	MA (mmol)	yield (g)	activity[b]	X_{MA}[c] (mol %)	M_n[d] (kDa)	PDI[d]	$N_{br/1000}$[e]
1	**Ni1**	5	0.60	15	0.5	4.5	1.6	73
2	**Ni2**	5	0.16	4	1.5	0.7	2.3	98
3	**Ni3**	5	0.10	2.5	7.5	0.7	1.9	128
4	**Ni4**	5	0.10	2.5	2.8	1.0	1.2	77
5	**Ni1**	10	0.10	2.5	1.9	4.2	1.8	66
6[f]	**Ni2**	5	0.30	7.5	6.1	0.8	1.6	125

[a]Polymerization conditions: Ni catalyst = 10 μmol dissolved in 2 mL of *o*-dichlorobenzene; cocatalyst = $AlEt_2Cl$ (2 mmol); solvent = 50 mL of toluene; T = 40 °C, P_E = 6 atm, time 4 h. [b]Activity in kg of copolymer/$mol_{(Ni)}$ h. [c]Incorporation of MA in the copolymer determined by ^1H NMR. [d]Determined by size exclusion chromatography (SEC) vs polystyrene standards. [e]Determined by ^1H NMR. [f]Instead of $AlEt_2Cl$, the cocatalyst was a mixture of $AlMe_3$ (1 mmol), $B(C_6F_5)_3$ (15 μmol) and $[Ph_3C][B((C_6F_5)_4]$ (15 μmol).

Table 2. Ethylene-Methyl Acrylate Copolymerizations by Complexes Ni1−Ni4 under Higher Ethylene Pressure[a]

run (sample)	Ni catalyst	MA (mmol)	P_E (atm)	yield (g)	X_{MA}[b] (mol %)	M_n[c] (kDa)	PDI[c]	$N_{br/1000}$[d]
7	**Ni1**	5	30	8.94[e]	0.2	11.7	1.3	68
8	**Ni1**	5	10	5.32[e]	0.3	9.3	1.4	70
9	**Ni1**		30	11.0		3.1	1.4	71
10	**Ni1**	5	0	0.02	100	0.3	1.2	
11	**Ni2**	5	30	6.45	0.3	1.2	1.7	141
12	**Ni2**	10	30	0.17	0.6	0.9	1.7	97
13	**Ni2**	5	10	1.04	1.2	1.1	1.5	128
14	**Ni2**	10	10	0.15	2.6	1.9	1.2	130
15	**Ni3**	5	30	0.14	7.8	0.3	1.1	66
16	**Ni3**	2.5	50	0.12	2.4	4.8	1.4	66
17	**Ni3**	5	10	0.10	17.7	0.3	1.0	18
18	**Ni3**[f]	5	10	0.10	35.0	0.3	1.2	91
19	**Ni3**[g]	5	30	0.17	11.0	0.3	1.1	124
20	**Ni4**	5	30	0.36	1.0	0.9	1.2	43

[a]Polymerization conditions: Ni catalyst = 10 μmol dissolved in 2 mL of dichloromethane; cocatalyst = $AlEt_2Cl$ (2 mmol); solvent = 20 mL toluene; T = 40 °C, time 20 h. [b]Incorporation of MA in the copolymer determined by ^1H NMR. [c]Determined by SEC vs polystyrene standards. [d]Determined by ^1H NMR. [e]A waxy polymer precipitated when the reaction mixture was poured into methanol; only traces of the oily fraction was recovered from the methanol solution. [f]Instead of $AlEt_2Cl$, the cocatalyst was a mixture of $AlMe_3$ (1 mmol), $B(C_6F_5)_3$ (15 μmol), and $[Ph_3C][B((C_6F_5)_4]$ (15 μmol). [g]The Ni catalyst was dissolved in 2 mL of *o*-dichlorobenzene instead of dichloromethane.

equiv of $AlEt_2Cl$, at 40 °C, under variable conditions of ethylene pressure and methyl acrylate concentrations. The complexes were initially compared under 6 atm of ethylene and [MA] = 0.1 M (Table 1, runs 1−4), resulting in any case in the production of oily products, which did not precipitate when the reaction mixture was poured into acidified methanol, and were recovered by extraction with hexane/water as described in the Experimental Section. The apparent catalyst activities decrease in the order **Ni1** > **Ni2** > **Ni3** ∼ **Ni4**, paralleling the decreasing steric bulk of the ligands. Accordingly, the incorporation of MA in the copolymers, as determined by NMR analysis (v. infra), follows the opposite trend, increasing from 0.5% for **Ni1** to 1.5% for **Ni2** to 2.8% for **Ni4** to 7.5% for **Ni3**, as expected if coordination and insertion of MA slow down the polymerization. Increasing the MA concentration in the reaction mixture resulted in a decrease in productivity and an increase in MA incorporation (Table 1, Cf. runs 1 and 5).

As mentioned in the Introduction section,[26,27] activation of [α-diimine-$NiBr_2$] complexes with mixtures of $AlMe_3$ and B-based ionizing cocatalysts, such as $B(C_6F_5)_3$ and $[Ph_3C][B(C_6F_5)_4]$, is more efficient than $AlEt_2Cl$ for the copolymerization of ethylene with vinyltrialkoxysilanes. Following this suggestion, we tested complex **Ni2** after activation with $AlMe_3$ (100 equiv)/$B(C_6F_5)_3$ (1.5 equiv)/$[Ph_3C][B(C_6F_5)_4]$ (1.5 equiv), resulting in both higher productivity and increased MA incorporation (Cf. run 6 vs run 2, Table 1) but lower selectivity in the mode of MA insertion (see below).

SEC analysis of the copolymer samples showed that those produced by complexes **Ni2**−**Ni4** have very low M_n (≤1 kDa), while the samples produced by complex **Ni1** have significantly higher M_n (4.5 kDa). The polydispersities are rather narrow, ranging between 1.2 and 2.3.

Subsequently, several other copolymerization runs were performed for longer time (20 h) under higher ethylene pressures in a stainless-steel autoclave, allowing us to obtain a wide range of productivities and copolymer compositions (Table 2).

Under the latter conditions, using [MA] = 0.25 M and either 30 or 10 atm of ethylene, precatalyst **Ni1** produced waxy polymers, which precipitated when the reaction mixture was poured into acidified methanol (runs 7 and 8, Table 2). NMR analysis showed that these samples consist of branched PE with MA incorporation 0.2% for sample 7 and 0.3% for sample 8. Only traces of oily copolymer fractions were recovered from the reaction solutions. An ethylene homopolymerization run was performed under the same conditions as that of run 7 without adding MA (run 9, Table 2), but in this case no solid precipitated in methanol, while 11.0 g of oily polymer was recovered from the solution. Comparison of the polymer samples produced in the presence and in the absence of MA under otherwise identical conditions showed that the former has a higher molecular weight (11.7 vs 3.1 kDa) and a

https://dx.doi.org/10.1021/acs.macromol.0c01703
Macromolecules 2020, 53, 9294−9305

slightly lower branching content with respect to the latter (68 vs 71 branches per 1000 C's). A possible explanation of these unexpected results is that, under these conditions, κ-O coordination of MA to the Ni catalyst site preferentially occurs vs π-coordination, disfavoring the β-agostic alkyl Ni intermediates which are precursors of both chain termination and chain running, thus resulting in polymers with less branching, higher molecular weight, and lower MA incorporation.

Precatalyst **Ni2** afforded 6.45 g of methanol-soluble oily copolymer with 0.3% MA incorporation using [MA] = 0.25 M and 30 atm of ethylene (run 11, Table 2); doubling up MA concentration under the same ethylene pressure resulted in a twofold increased incorporation but with a severe decrease in the productivity (run 12, Table 2). A reasonable trade-off between productivity and incorporation was achieved using [MA] = 0.25 M and 10 atm of ethylene (run 13, Table 2), while a higher MA incorporation could be achieved using [MA] = 0.5 M and 10 atm of ethylene (see run 14, Table 2), always associated with a remarkable decrease in the productivity.

As already observed, precatalyst **Ni3** was much more inclined to MA incorporation, allowing the production of copolymers with MA contents ranging from 2.4% using [MA] = 0.125 M and P_E = 50 atm up to 17.7% using [MA] = 0.5 M and P_E = 10 atm but in all cases with low yields (see runs 15, 16, 17, Table 2). Under the latter conditions, activation with $AlMe_3/B(C_6F_5)_3/[Ph_3C][B(C_6F_5)_4]$ resulted in the production of a copolymer with a much higher MA content (35.0%, run 18, Table 2), as already found for catalyst **Ni2** (runs 2 and 6, Table 1), even though under different reaction conditions. The corresponding ketimino derivative **Ni4** was less able to incorporate MA and consequently, under the same conditions, produced a higher yield (Cf. runs 15 and 20, Table 2).

As suggested by the reviewers, two control experiments of MA homopolymerization were performed under conditions similar to those of run 9 by using either **Ni1** activated by $AlEt_2Cl$, (see run 10, Table 2) or $AlMe_3/B(C_6F_5)_3/[Ph_3C]$-$[B(C_6F_5)_4]$ without Ni, resulting in the production of a few mg of low-molecular weight poly(methylacrylates) in both cases. ^{1}H and ^{13}C NMR characterization of the latter samples and, for comparison, of a poly(methylacrylate) sample prepared by O_2-initiated radical polymerization (see Figures S5 and S6) showed remarkable differences among the three MA homopolymers and between them and the ethylene/MA copolymers (see below).

The obtained copolymers were analyzed by ^{1}H and ^{13}C NMR spectroscopy. The ^{1}H NMR spectrum of sample 3 is shown in Figure 1: in addition to the resonances of hyperbranched homo-PE, including those of the unsaturated vinylene, allyl, and vinylidene protons,[39] a main rather broad resonance centered at δ 3.67 is detected in the region of methoxy protons. On the basis of the ^{13}C NMR analysis (v. infra) it is attributed to methoxy protons of MA units inserted *in-chain* (Table 3, fragment *a*); minor resonances in the methoxy regions are detected at δ 3.70 and 3.77 ppm, while broad resonances of allylic protons and methylenic groups closer to the ester functionality are observed between 2.20−2.66 and at 1.60 ppm. Minor low-field resonances, evidenced with a magnification of 20 times with respect to the other signals, are also detected between δ 12.24 and 12.42 ppm (v. infra and Figure 5 for the assignments).

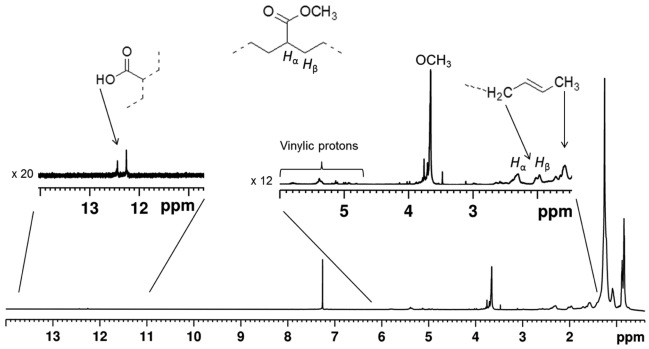

Figure 1. ^{1}H NMR spectrum ($CDCl_3$, T = 298 K) of the copolymer sample of run 3.

The ^{1}H NMR spectra of the samples 1−5 of Table 1 are very similar, aside from the obvious different resonance intensities due to the higher or lower content of MA in the copolymers, thus indicating that the different substituents on the pyridylimino ligand do not affect the kind of incorporation of MA but only its inserted amount.

Unexpectedly, ^{1}H NMR analysis of the copolymer samples reported in Table 2, as well as of sample 6, showed that the relative intensities of the three main peaks due to the methoxy groups vary significantly (Figure 2). The methoxy regions of the spectra of three representative samples prepared with the same precatalyst **Ni2** under different conditions, i.e., in run 2 (Table 1), run 14 (Table 2), and run 6 (Table 1), are compared as shown in Figure 2. It is apparent that while for sample 2 the main resonance is that at δ 3.67 (as in the previously discussed sample 3), for sample 6 the main signal is that at 3.77 ppm, whereas for sample 14 the three methoxy resonances between 3.67 and 3.77 ppm show comparable intensities. Accordingly, the ^{13}C NMR spectra (Figure 3) show different patterns of resonances for the different samples, thus indicating a different mode of MA incorporation in the obtained macromolecules.

In the carbonyl region of the spectrum of sample 3 (Figure 3, lower trace) two main broad resonances are observed at δ 176.7 and 176.4 ppm; resonances at δ 51.5 are observed for the methoxy group and at 45.4 and 43.6 ppm for the methine carbons of the MA units. On the basis of literature data[42] and multidimensional NMR experiments (see below) these resonances are assigned to MA units inserted *in-chain* (fragment *a*): the occurrence of two broad carbonyl resonances is reasonably due to both the low-molecular weight and the hyperbranched structure of the macromolecules, the latter being at the origin of the small variations in chemical shift with respect to the literature data (176.7 and 176.4 vs 177.17 ppm; 51.5 vs 51.4 ppm; and 45.4 and 43.6 vs 45.9 ppm).

The ^{13}C-NMR spectrum of sample 15 (Figure 3, middle trace) appears much more complicated: in addition to the peaks due to the MA units inserted *in-chain* mentioned above, at least four sharp resonances of comparable intensities are found at δ 175.5 (split), 174.5, 174.3, and 173.0 (split). Multiple less intense peaks are observed between 170.4−169.8 ppm and at δ 167.2 ppm. Minor resonances are also observed at δ 206.8, 205.7, and 194.9 (Figure S7).

Thanks to a thorough NMR investigation performed mainly by ^{1}H,^{13}C-HSQC, and ^{1}H,^{13}C-HMBC experiments, it was possible to identify the diverse fragments containing the polar monomer. The signals in the range 169−178 ppm are due to

https://dx.doi.org/10.1021/acs.macromol.0c01703
Macromolecules 2020, 53, 9294−9305

Table 3. Molecular Fragments Containing MA in the Synthesized E-MA Copolymers with the Corresponding ^{1}H and ^{13}C NMR Resonance Assignments[a]

	Fragments	NMR Shifts		
		n	^{1}H	^{13}C
a	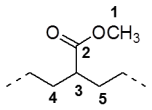	**1**	3.67	51.5
		2	-	176.7, 176.4
		3	2.33	45.4
		4	1.58	34.6
		5	1.40	32.2
b	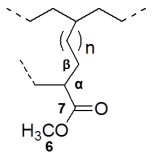	**6**	3.77	51.6
		7	-	172.9
		α	2.32	43.4
		β	1.65	24.5
c	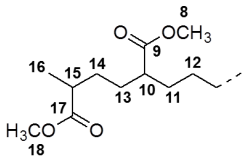	**8**	3.47	55.2
		9	-	205.7
		10	2.38	49.1
		11	2.54	25.0
		12	1.08	27.0
		13	1.17	36.1
		14	1.76	34.5
		15	2.50	39.2
		16	1.04	14.1
		17	-	206.8
		18	3.72	52.5
d	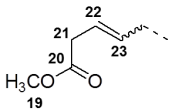	**19**	3.70	51.6
		20	-	194.8
		21	1.38	32.7
		22	6.50/5.86	134.7/139.3
		23	6.50/5.86	134.7/139.3
e	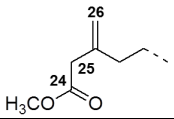	**24**	-	194.8
		25	1.38	32.7
		26	6.34	129.8
f	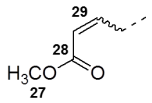	**27**	3.73	52.2
		28	-	167.2
		29	6.9/7.0	148.9
g	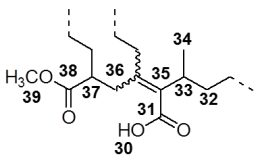	**30**	12.24	-
		31	-	174.5
		32	2.54/2.38	25.2
		33	2.37	37.2
		34	1.17	17.3
		35	-	95.6
		36	2.26/2.63	25.7
		37	2.37	37.2
		38	-	175.4
		39	3.70	51.9
h	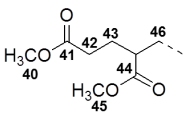	**40**	3.77	51.6
		41	-	169.8/170.4
		42	2.25	25.7
		43	2.03	27.2
		44	-	169.8/170.4
		45	3.77	51.6
		46	1.84	30.5

[a]NMR spectra recorded in $CDCl_3$ at T = 298 K.

the carbonyl groups of MA units inserted both *in-chain* and at the end of the branches (fragment *b*, Table 3), in agreement with the literature and as confirmed by the cross peaks in both the $^{1}H,^{13}C$-HMBC (Figure 4) and the $^{1}H,^{13}C$-HSQC (Figure S8) spectra.

In addition, in the $^{1}H,^{13}C$ −HMBC spectrum (Figure 5) the carbonyl peak at 174.5 ppm shows two cross peaks with the signals at 12.24 and 12.42 ppm in the ^{1}H NMR spectrum. These latter peaks also correlate with a resonance at 96.2 ppm in the ^{13}C NMR spectrum that, in turn, does not show any correlation peak in the $^{1}H,^{13}C$-HSQC spectrum (Figure S9), thus suggesting that it is originated by a quaternary carbon atom. A closer inspection of ^{1}H NMR spectra of all samples points out that the signals around 12 ppm, even though of very low intensity, are always present. This NMR analysis indicates that these signals are due to an acrylic acid moiety (Table 3, fragment *g*) resulting from hydrolysis of the ester functionality taking place either during the polymerization

https://dx.doi.org/10.1021/acs.macromol.0c01703
Macromolecules 2020, 53, 9294−9305

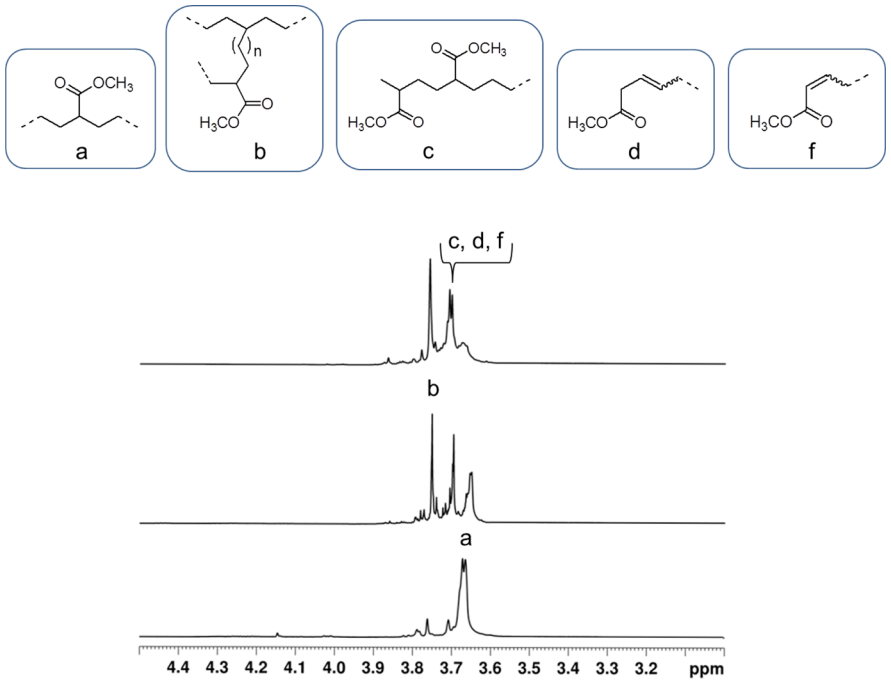

Figure 2. Methoxy regions of the ^{1}H NMR spectra ($CDCl_3$, T = 298 K) of the copolymer samples of runs 2 (lower trace), 14 (middle trace), and 6 (upper trace).

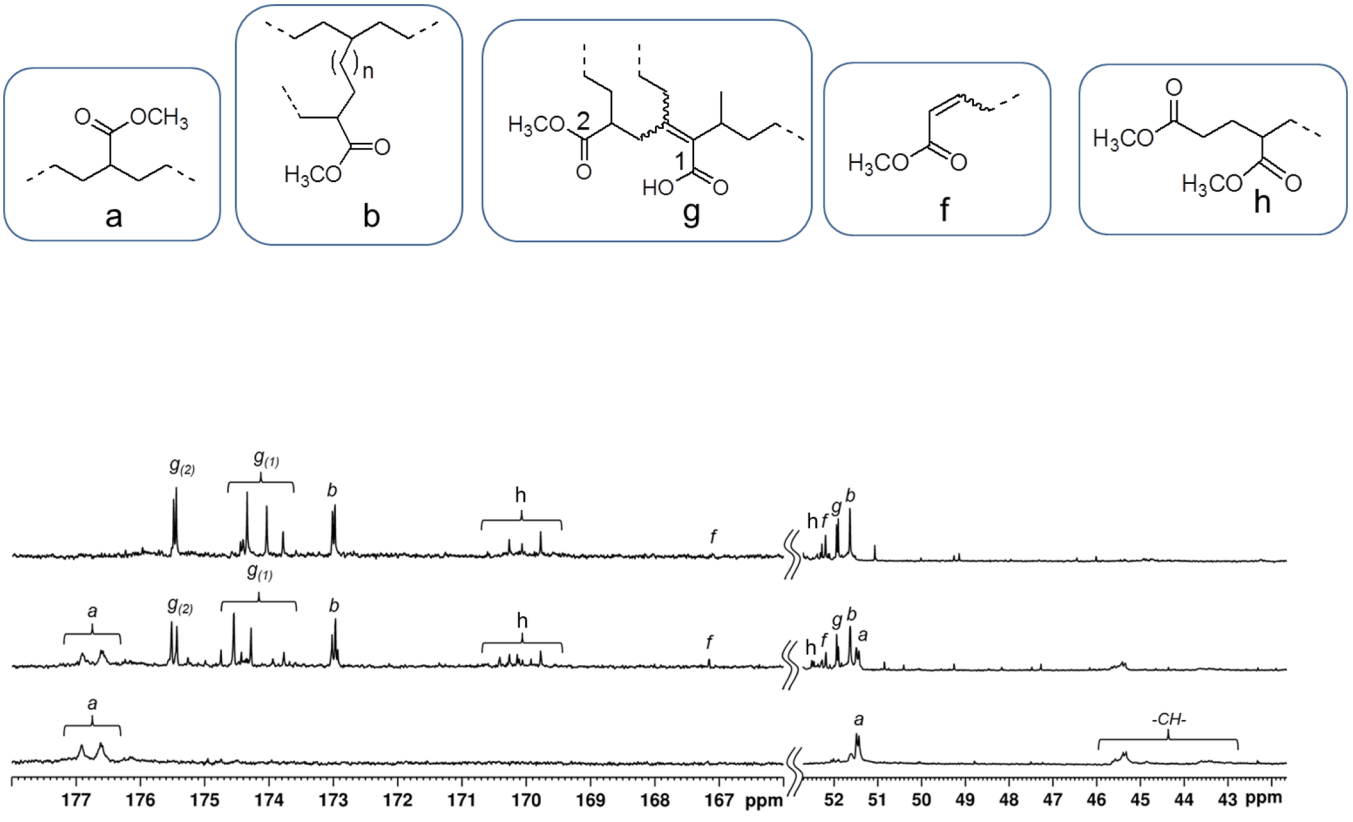

Figure 3. Carbonyl, methoxy, and C═O substituted methine regions of the ^{13}C NMR spectra ($CDCl_3$, T = 298 K) of copolymer samples of runs 3 (lower trace), 15 (middle trace), and 6 (upper trace).

process or during the work up, although also recovering the copolymer by simply distilling off the volatiles directly from the polymerization mixture resulted in the formation of some acrylic acid −OH. It is reported in the literature that Ni complexes catalyze the hydrolysis of ester groups.[43]

Starting from the resonances of the carbonyl groups at 206.8 and 205.7 ppm through the correlation peaks in the ^{1}H,^{13}C-HMBC spectrum (Figure 6), the fragment featuring the alternating MA-E-MA sequence was recognized (Table 3, fragment *c*). In a similar way the cross peaks related to the

https://dx.doi.org/10.1021/acs.macromol.0c01703
Macromolecules 2020, 53, 9294−9305

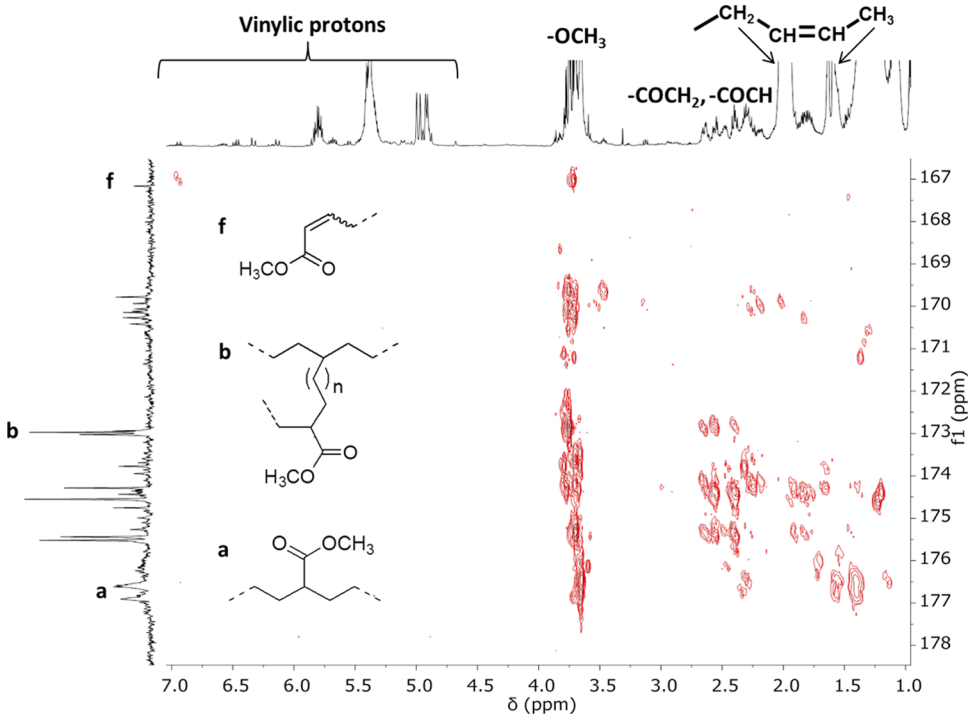

Figure 4. Section of the $^{1}H,^{13}C$ −HMBC spectrum ($CDCl_3$, T = 298 K) of sample 15. ^{1}H scale: all the required signals; ^{13}C scale: carbonyl signals only, range 167−178 ppm.

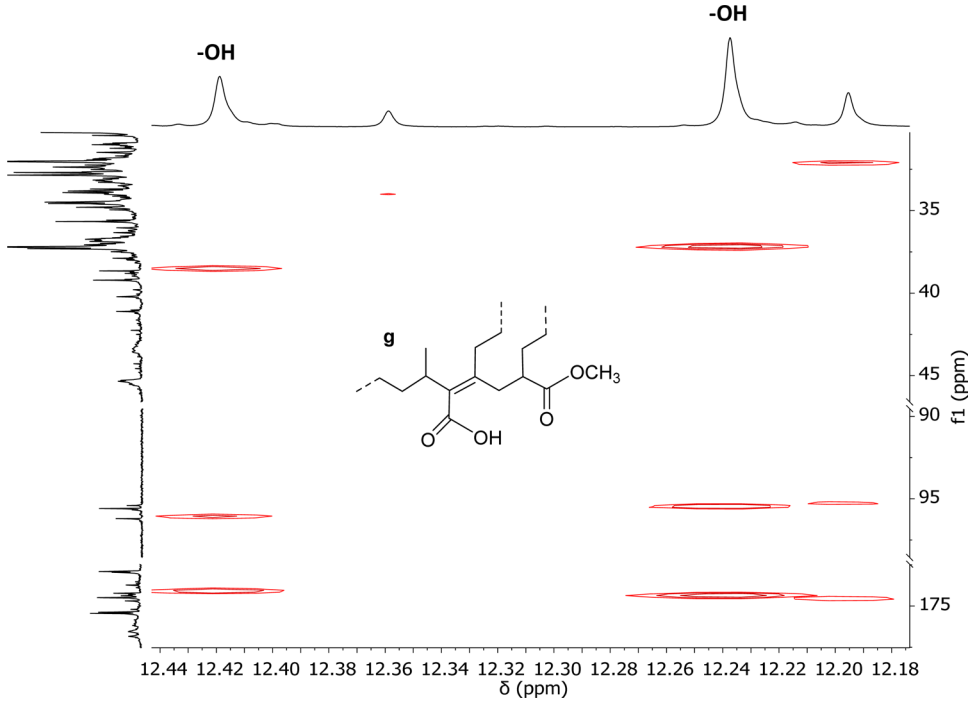

Figure 5. Section of the $^{1}H,^{13}C$ −HMBC spectrum ($CDCl_3$, T = 298 K) of sample 17. ^{1}H scale: signals at 12.42 and 12.24 ppm (magnified 20 times with respect to the other signals); ^{13}C scale: all the required signals. The two minor resonances detected are reasonably due to similar acrylic acid fragments in slightly different environments.

carbonyl at 194.8 ppm indicate the presence of two isomeric unsaturated moieties assigned to fragments *d* and *e* (Table 3, Figure S8).

As far as the minor peaks in the range 170.4−169.8 ppm are concerned (Figure 3, middle trace), the $^{1}H,^{13}C$ −HMBC spectrum shows cross peaks with the methoxy signal at 3.77 ppm and with the signals of methylenic protons around 2.25, 2.03, and 1.84 ppm. The assignments of these signals resulted to be rather difficult and they were attributed to the molecular fragment having two consecutive MA units (fragment *h*, Table 3). This attribution is also confirmed by analogy with the ^{13}C NMR spectrum of the poly(MA) obtained with **Ni1** (see Figure S6).

https://dx.doi.org/10.1021/acs.macromol.0c01703
Macromolecules 2020, 53, 9294−9305

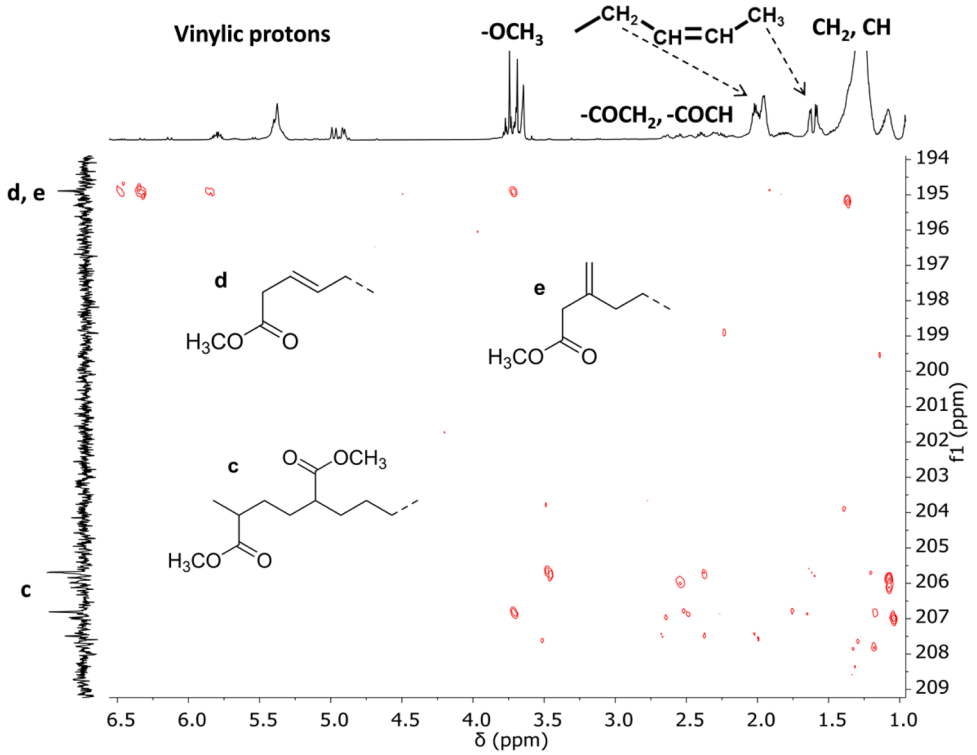

Figure 6. Section of the $^{1}H,^{13}C$ −HMBC spectrum ($CDCl_3$, T = 298 K) of sample 15. ^{1}H scale: all the required signals; ^{13}C scale: carbonyl signals only, range over 194 ppm.

Finally, in agreement with the literature,[32] the carbonyl group that resonates at 167.2 ppm was attributed to the fragment resulting from the *β*-hydrogen elimination (BHE) taking place immediately after the insertion of the polar monomer (Figure 4; Table 3, fragment *f*).

The ^{13}C NMR spectra of sample 6 (Figure 3, upper trace) show all the resonances discussed for sample 15, except for those attributable to the *in-chain* MA units. Therefore, the enchainment modes of MA in the three copolymer samples shown in Figure 3 (which are representative of all the different samples reported in Tables 1 and 2) range from "*in-chain* only" of sample 3 to "everywhere but *in-chain*" of sample 6. The ^{1}H and ^{13}C NMR resonance assignments for all the MA-containing fragments are summarized in Table 3. The comparison with the ^{1}H and ^{13}C NMR spectra of poly(MA) obtained in the control experiments (Figures S5 and S6) allows us to identify fragments *a, b,* and *d*–*f* as belonging to the ethylene/MA copolymers only, whereas fragments *c, h,* and *g* are also present in poly(MA) produced with **Ni1**. Instead, no fragment is shared with the homopolymers synthesized either with the radical or the $AlMe_3/B(C_6F_5)_3/[Ph_3C][B(C_6F_5)_4]$-initiated polymerization.

This NMR analysis indicates that the nickel catalysts under investigation lead to real ethylene/MA copolymers that are obtained as hyperbranched macromolecules with MA inserted in diverse molecular fragments. As reported very recently, the *in-chain* incorporation of MA is possible also when the chain walking mechanism is active.[44] Therefore, on the basis of the above considerations, starting from intermediate **I**, originated by MA insertion into the Ni-alkyl bond with a secondary regiochemistry, several parallel reaction pathways might be operative to explain the different manners of MA incorporation (Scheme 2):

i. coordination-insertion of several ethylene units leads to fragment *a*;
ii. the chain walking process leads to fragment *b*;
iii. on **I** BHE can occur leading to fragment *f* and a Ni-H species;
iv. fragment *d* is originated by BHE taking place after MA insertion and chain walking;
v. similarly, fragment *e* is the result of BHE taking place as that in pathway iv but on a methyl branch.
vi. fragment *c* is obtained starting from the Ni-H intermediate on which coordination-insertion of MA with secondary regiochemistry takes place followed by coordination-insertion of ethylene and of another molecule of MA leading to the growing copolymer chain; whereas fragment *h* is the result of two consecutive insertions of MA molecules with primary regiochemistry, the first of the two occurring on the Ni-H intermediate; and
vii. fragment *g* is analogous to fragment *c* and its formation implies the occurrence of BHE during chain walking plus hydrolysis of the ester group.

The fact that the nickel catalysts under investigation are also able to catalyze MA homopolymerization, even though with a very low yield, supports our hypothesis that the consecutive insertion of two MA units is possible even under the copolymerization conditions. However, the concurrent formation of traces of poly(MA) cannot be ruled out.

The correlation of the variety of structures observed in the modes of MA enchainment with the catalysts and/or the reaction conditions is not straightforward. For example, the samples whose ^{1}H NMR spectra are shown in Figure 2 were prepared with the same Ni precatalyst, indicating that the ligand structure is not relevant for this aspect. On the

https://dx.doi.org/10.1021/acs.macromol.0c01703
Macromolecules 2020, 53, 9294−9305

Scheme 2. Possible Reaction Pathways That Lead to the Detected Molecular Fragments *a*–*g*[a]

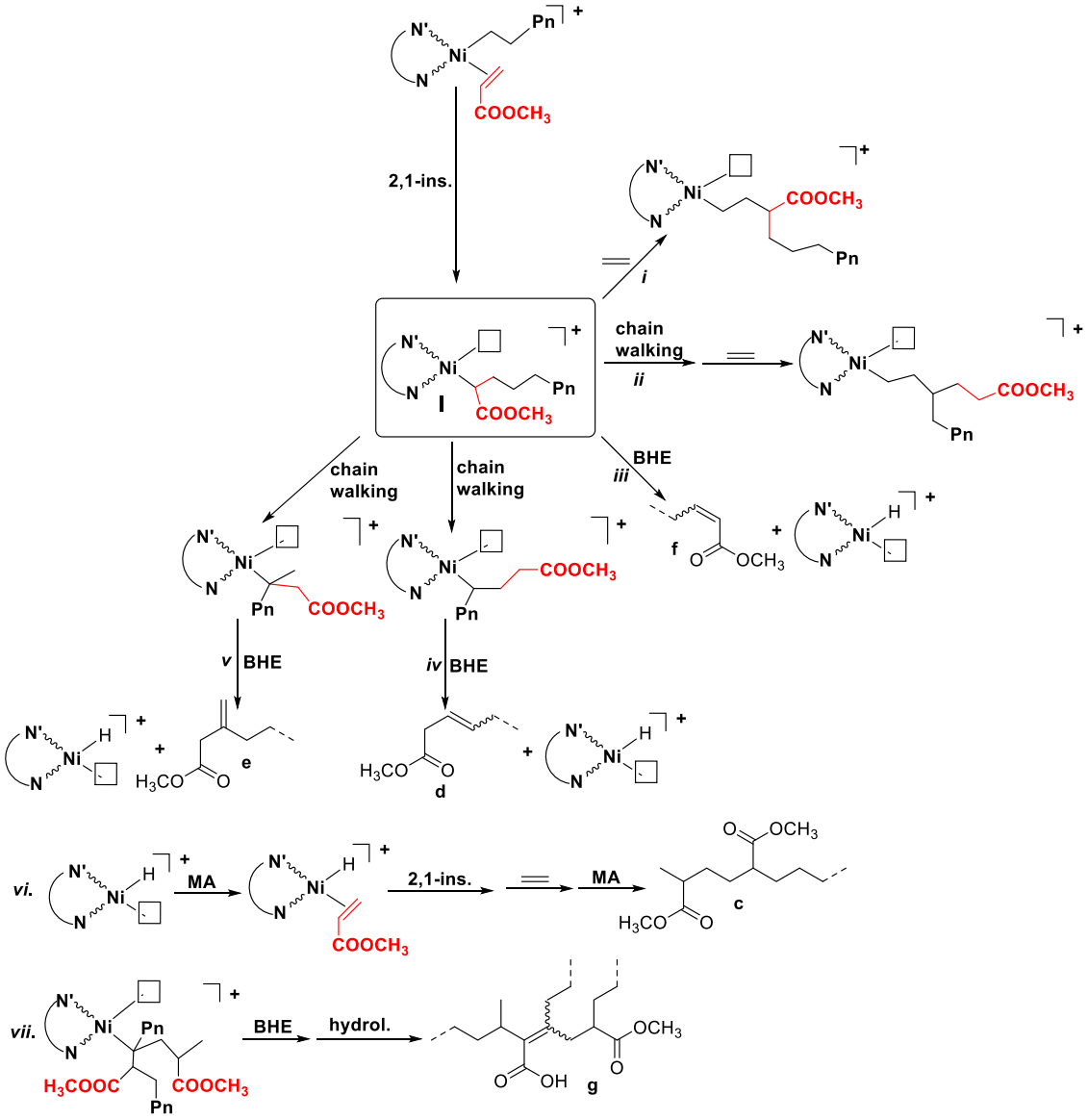

[a]P_n = growing polymer chain

contrary, it is apparent that the mode of activation plays a significant role: for samples 2 and 6, obtained with the same precatalyst under the same reaction conditions but with a different activation mode, the NMR analysis indicates that when the activation is performed using $AlMe_3/B(C_6F_5)_3/[Ph_3C][B(C_6F_5)_4]$ (as for sample 6) in place of $AlEt_2Cl$ (as for sample 2), the polar monomer is preferentially located at the end of the branches rather than *in-chain*.

The procedures used to prepare the samples of Tables 1 and 2, showing different modes of MA enchainment even using the same Ni precatalyst and $AlEt_2Cl$ cocatalyst, differ for ethylene pressures, methyl acrylate concentration, and the type of solvent used to dissolve the Ni complexes, i. e, *o*-dichlorobenzene for the runs of Table 1 vs dichloromethane for the runs of Table 2. As a matter of fact, a copolymerization run performed under the same conditions of run 15 but dissolving the Ni precatalyst **Ni3** in *o*-dichlorobenzene instead of dichloromethane afforded a copolymer with a high selectivity for *in-chain* incorporation of MA (run 19, Figures S11 and S12), having a microstructure similar to that of the copolymer obtained under 6 atm of ethylene (Table 1, run 3).

Overall, these data suggest that the mode of enchainment of MA is affected by both the activating agent and the solvent used to dissolve the Ni precatalyst. That is, when the activating agent is $AlEt_2Cl$, copolymers with MA preferentially inserted *in-chain* are obtained if the Ni complex is dissolved in *o*-dichlorobenzene, whereas copolymers with a variety of MA enchainments are produced when the reaction is carried out by dissolving the precatalyst in dichloromethane. Activation by $AlMe_3/B(C_6F_5)_3/[Ph_3C][B(C_6F_5)_4]$ also results in copolymers with a nonselective MA mode of incorporation, with total suppression of the *in-chain* units. Our results also suggest that the activation either with $AlEt_2Cl$ in dichloromethane or with $AlMe_3/B(C_6F_5)_3/[Ph_3C][B(C_6F_5)_4]$ leads to active species which are prone to give β-hydride elimination reactions after the acrylate insertion, originating fragments *d*, *e*, and *f* (Table 3) and the Ni-H intermediate that is able to

https://dx.doi.org/10.1021/acs.macromol.0c01703
Macromolecules 2020, 53, 9294–9305

insert a molecule of MA starting a new catalytic cycle, as demonstrated by the detection of fragments *c* and *h* (Table 3).

Solvent effects on the microstructure of ethylene-methyl acrylate copolymers were recently reported for α-diimine Pd catalysts[42] showing a lower selective enchainment when the copolymerization is carried out in dichloromethane with respect to the use of trifluoroethanol as the reaction medium.

The effect of the different activating agents on the productivity was reported by Brookhart in the Ni-catalyzed copolymerization of ethylene with vinyltrialkoxysilanes, but no variation on the copolymer microstructure was observed.[26,27]

CONCLUSIONS

We have synthesized four Ni(II) complexes bearing pyridylimine (either aldimine or ketimine) ligands, differing for the substituent in position 6 of the pyridine ring and for the group in *ortho* position on the aryl ring bound to the imino nitrogen. These complexes, in the presence of a proper activating agent, were found to generate active catalysts for the ethylene-methyl acrylate copolymerization leading to hyperbranched copolymers with the polar monomer inserted in a variety of modes, some of which have been observed and characterized for the first time.

The nature of the pyridylimine ligand determines catalyst activity, polymer molecular weight, and content of inserted MA. In particular, complex **Ni1** having the most hindered ligand of the series generates the most active catalyst yielding the copolymer with the highest molecular weight but the lowest content of the polar monomer. Instead, complex **Ni3** having the less hindered pyridine ring gives the copolymer with the highest incorporation of MA.

The ligand nature does not affect the manner of incorporation of MA that is dictated by both the activating agent and the solvent used to dissolve the nickel precatalyst: selective *in-chain* MA insertion occurs when the activator is $AlEt_2Cl$ and the precatalyst is dissolved in *o*-dichlorobenzene, while a variety of insertion modes occur in the presence of dichloromethane or $AlMe_3/B(C_6F_5)_3/[Ph_3C][B(C_6F_5)_4]$ cocatalyst.

In conclusion, we have demonstrated that Ni(II) complexes with very simple and versatile ancillary ligands generate active catalysts for the copolymerization of ethylene with methyl acrylate, affording low-molecular weight highly branched functionalized polyolefin oils, which could be of interest, e.g., for applications as base stocks for synthetic lubricants or as interface active agents.[45]

EXPERIMENTAL SECTION

General Conditions. All procedures sensitive to air or moisture were performed under a nitrogen atmosphere using standard Schlenk techniques. Glassware used were dried in an oven at 120 °C overnight and exposed three times to vacuum−nitrogen cycles. Solvents were dried by refluxing with a dryng agent (CaH_2 for dichloromethane and metallic sodium for toluene and *o*-dichlorobenzene) and distillation under nitrogen. Deuterated solvents were purchased from Aldrich and stored in a glovebox over 3 Å molecular sieves before use. All other reagents were purchased from Aldrich and used as received. Ethylene was purchased from SON and used without further purification.

The NMR spectra were recorded on a Bruker Advance 400, a Bruker 600 MHz Ascend 3 HD spectrometers, and a Varian 500 MHz.

^{1}H NMR spectra are referenced using the residual solvent peak at δ 7.26 for $CDCl_3$. ^{13}C NMR spectra are referenced using the residual solvent peak at δ 77.16 for $CDCl_3$.

The molecular weights (M_n and M_w) and the molecular mass distribution (M_w/M_n) of the polymer samples were measured by SEC at 30 °C, using THF as solvent, an eluent flow rate of 1 mL/min, and narrow polystyrene standards as reference. The measurements were performed on a Waters 1525 binary system equipped with a Waters 2414 RI detector using four Styragel columns (range 1000−1000 000 A).

High-resolution mass spectroscopy (HRMS) was carried out using a Bruker SolariX XR FT-ICR mass spectrometer (Bruker Daltonik GmbH, Bremen, Germany) equipped with a 7 T refrigerated actively shielded superconducting magnet (Bruker Biospin, Wissembourg, France). The samples were ionized in positive ion mode using an ESI ion source (Bruker altonik GmbH, Bremen, Germany). The mass range was set to *m/z* 150−3000. Mass calibration: The mass spectra were calibrated externally using a NaTFA solution in positive ion mode. A linear calibration was applied.

Synthesis of Ligands and Complexes. Ligands $\mathbf{L^1}$-$\mathbf{L^4}$ and complexes **Ni3**-**Ni4** were synthesized according to previously reported procedures[34,35,40,41] (see the Supporting Information for details). New complexes **Ni1**-**Ni2** were prepared from [(DME)-$NiBr_2$] and the corresponding ligand in dichloromethane. The reaction mixture was stirred at room temperature for 24 h. The solvent was removed under vacuum and the residues were washed with dry hexane and dried. HRMS (ESI+) *m/z* calcd for **Ni1**: 603.05; found: 523.15 [$\mathbf{L^1}$Ni-Br$^+$]. HRMS (ESI+) *m/z* calcd for **Ni2**: 532.92; found 453.03 [$\mathbf{L^2}$Ni-Br$^+$].

General Procedure for Ethylene Homo- and Copolymerizations at 6 atm. Ethylene homo- and copolymerizations at 6 atm were all carried out in a 250 mL Büchi glass autoclave equipped with a mechanical stirrer and a temperature probe. The reactor was kept under vacuum overnight at 80 °C. In a typical run, the reactor vessel was charged under a nitrogen atmosphere with 50 mL of toluene solution containing the Ni catalyst, the cocatalyst, and, for copolymerizations, the MA comonomer. Then, it was pressurized with ethylene and vented three times. The mixture was stirred at 40 °C under constant ethylene pressure for 4 h and then the autoclave was vented and the reaction mixture was poured into acidified methanol. The resulting solution was treated with hexane and water, then the organic layer was dried over $MgSO_4$, filtered, and the volatiles were distilled off in a rotavapor. The resulting oily residue was dried in vacuo overnight at 80 °C.

General Procedure for Ethylene-Methyl Acrylate Copolymerization at Higher Pressures. Ethylene copolymerizations at high pressures (10−50 atm) were carried out in a stainless-steel autoclave equipped with a magnetic stirrer. The reactor was first dried overnight at 120 °C in an oven, cooled under vacuum, then pressurized with ethylene, and vented three times. The reactor was thermostated at 40 °C, charged with 20 mL of toluene, the solution of cocatalyst, catalyst, and methyl acrylate, and then pressurized at the prescribed ethylene pressure. The mixture was stirred for 20 h under constant ethylene pressure and then poured into acidified methanol. The soluble copolymers were recovered as described above. Only in the case of runs 7 and 8, solid polymers precipitated in methanol and were recovered by filtration, washed with fresh methanol, and dried in vacuo at 80 °C overnight.

ASSOCIATED CONTENT

Supporting Information

The Supporting Information is available free of charge at https://pubs.acs.org/doi/10.1021/acs.macromol.0c01703.

Synthesis and characterization of ligands, HR ESI Mass spectra of complexes, and ^{1}H NMR, ^{13}C NMR, and ^{1}H,^{13}C −HSQC NMR spectra of polymers (PDF)

https://dx.doi.org/10.1021/acs.macromol.0c01703
Macromolecules 2020, 53, 9294−9305

AUTHOR INFORMATION

Corresponding Authors

Barbara Milani − *Dipartimento di Scienze Chimiche e Farmaceutiche, Università di Trieste, 34127 Trieste, Italy;* orcid.org/0000-0002-4466-7566; Email: milaniba@units.it

Claudio Pellecchia − *Dipartimento di Chimica e Biologia "A. Zambelli", Università di Salerno, 84084 Fisciano, Salerno, Italy;* orcid.org/0000-0003-4358-1776; Email: cpellecchia@unisa.it

Authors

Zeinab Saki − *Dipartimento di Chimica e Biologia "A. Zambelli", Università di Salerno, 84084 Fisciano, Salerno, Italy*

Ilaria D'Auria − *Dipartimento di Chimica e Biologia "A. Zambelli", Università di Salerno, 84084 Fisciano, Salerno, Italy;* orcid.org/0000-0002-3561-012X

Anna Dall'Anese − *Dipartimento di Scienze Chimiche e Farmaceutiche, Università di Trieste, 34127 Trieste, Italy*

Complete contact information is available at: https://pubs.acs.org/10.1021/acs.macromol.0c01703

Notes

The authors declare no competing financial interest.

ACKNOWLEDGMENTS

This work was supported by Università degli Studi di Salerno (FARB 2017) and by Università degli Studi di Trieste (FRA 2018). The authors acknowledge the technical assistance of Dr. P. Iannece for MS measurements, Dr. M. Napoli for SEC analyses, and Dr. P. Oliva for NMR experiments.

REFERENCES

(1) Keyes, A.; Basbug Alhan, H. E.; Ordonez, E.; Ha, U.; Beezer, D. B.; Dau, H.; Liu, Y.-S.; Tsogtgerel, E.; Jones, G. R.; Harth, E. Olefins and Vinyl Polar Monomers: Bridging the Gap for Next Generation Materials. *Angew. Chem., Int. Ed.* **2019**, *58*, 12370−12391.

(2) Johnson, L. K.; Mecking, S.; Brookhart, M. Copolymerization of Ethylene and Propylene with Functionalized Vinyl Monomers by Palladium(II) Catalysts. *J. Am. Chem. Soc.* **1996**, *118*, 267−268.

(3) Mecking, S.; Johnson, L. K.; Wang, L.; Brookhart, M. Mechanistic Studies of the Palladium-Catalyzed Copolymerization of Ethylene and α-Olefins with Methyl Acrylate. *J. Am. Chem. Soc.* **1998**, *120*, 888−899.

(4) Drent, E.; van Dijk, R.; van Ginkel, R.; van Oort, B.; Pugh, R. I. Palladium catalysed copolymerisation of ethene with alkylacrylates: polar comonomer built into the linear polymer chain. *Chem. Commun.* **2002**, 744−745.

(5) Nakamura, A.; Anselment, T. M. J.; Claverie, J.; Goodall, B.; Jordan, R. F.; Mecking, S.; Rieger, B.; Sen, A.; van Leeuwen, P. W. N. M.; Nozaki, K. *Ortho*-Phosphinobenzenesulfonate: A Superb Ligand for Palladium-Catalyzed Coordination−Insertion Copolymerization of Polar Vinyl Monomers. *Acc. Chem. Res.* **2013**, *46*, 1438−1449.

(6) Guo, L.; Liu, W.; Chen, C. Late transition metal catalyzed α-olefin polymerization and copolymerization with polar monomers. *Mater. Chem. Front.* **2017**, *1*, 2487−2494.

(7) Wang, F.; Chen, C. A continuing legend: the Brookhart-type α-diimine nickel and palladium catalysts. *Polym. Chem.* **2019**, *10*, 2354−2369.

(8) Guo, L.; Gao, H.; Guan, Q.; Hu, H.; Deng, J.; Liu, J.; Liu, F.; Wu, Q. Substituent Effects of the Backbone in α-Diimine Palladium Catalysts on Homo- and Copolymerization of Ethylene with Methyl Acrylate. *Organometallics* **2012**, *31*, 6054−6062.

(9) Zhong, S.; Tan, Y.; Zhong, L.; Gao, J.; Liao, H.; Jiang, L.; Gao, H.; Wu, Q. Precision Synthesis of Ethylene and Polar Monomer Copolymers by Palladium-Catalyzed Living Coordination Copolymerization. *Macromolecules* **2017**, *50*, 5661.

(10) Dai, S.; Zhou, S.; Zhang, W.; Chen, C. Systematic Investigations of Ligand Steric Effects on α-Diimine Palladium Catalyzed Olefin Polymerization and Copolymerization. *Macromolecules* **2016**, *49*, 8855−8862.

(11) Zhai, F.; Solomon, J. B.; Jordan, R. F. Copolymerization of Ethylene with Acrylate Monomers by Amide-Functionalized α-Diimine Pd Catalysts. *Organometallics* **2017**, *36*, 1873−1879.

(12) Meduri, A.; Montini, T.; Ragaini, F.; Fornasiero, P.; Zangrando, E.; Milani, B. Palladium-Catalyzed Ethylene/Methyl Acrylate Cooligomerization: Effect of a New Nonsymmetric α-Diimine. *Chem. Cat. Chem.* **2013**, *5*, 1170−1183.

(13) Rosar, V.; Montini, T.; Balducci, G.; Zangrando, E.; Fornasiero, P.; Milani, B. Palladium-Catalyzed Ethylene/Methyl Acrylate Co-Oligomerization: The Effect of a New Nonsymmetrical α-Diimine with the 1,4-Diazabutadiene Skeleton. *Chem. Cat. Chem.* **2017**, *9*, 3402.

(14) Allen, K. E.; Campos, J.; Daugulis, O.; Brookhart, M. Living Polymerization of Ethylene and Copolymerization of Ethylene/Methyl Acrylate Using "Sandwich" Diimine Palladium Catalysts. *ACS Catal.* **2014**, *5*, 456−464.

(15) Liao, Y.; Zhang, Y.; Cui, L.; Mu, H.; Jian, Z. Pentiptycenyl Substituents in Insertion Polymerization with α-Diimine Nickel and Palladium Species. *Organometallics* **2019**, *38*, 2075−2083.

(16) Wang, R.; Zhao, M.; Chen, C. Influence of ligand second coordination sphere effects on the olefin (co)polymerization properties of α-diimine Pd(ii) catalysts. *Polym. Chem.* **2016**, *7*, 3933−3938.

(17) Carrow, B. P.; Nozaki, K. Synthesis of Functional Polyolefins Using Cationic Bisphosphine Monoxide-Palladium Complexes. *J. Am. Chem. Soc.* **2012**, *134*, 8802−8805.

(18) Contrella, N. D.; Sampson, J. R.; Jordan, R. F. Copolymerization of Ethylene and Methyl Acrylate by Cationic Palladium Catalysts That Contain Phosphine-Diethyl Phosphonate Ancillary Ligands. *Organometallics* **2014**, *33*, 3546−3555.

(19) Sui, X.; Dai, S.; Chen, C. Ethylene Polymerization and Copolymerization with Polar Monomers by Cationic Phosphine Phosphonic Amide Palladium Complexes. *ACS Catal.* **2015**, *5*, 5932−5937.

(20) Nakano, R.; Nozaki, K. Copolymerization of Propylene and Polar Monomers Using Pd/IzQO Catalysts. *J. Am. Chem. Soc.* **2015**, *137*, 10934−10937.

(21) Zhang, W.; Waddell, P. M.; Tiedemann, M. A.; Padilla, C. E.; Mei, J.; Chen, L.; Carrow, B. P. Electron-Rich Metal Cations Enable Synthesis of High Molecular Weight, Linear Functional Polyethylenes. *J. Am. Chem. Soc.* **2018**, *140*, 8841−8850.

(22) Ittel, S. D.; Johnson, L. K.; Brookhart, M. Late-Metal Catalysts for Ethylene Homo- and Copolymerization. *Chem. Rev.* **2000**, *100*, 1169−1203.

(23) Mu, H.; Pan, L.; Song, D.; Li, Y. Neutral Nickel Catalysts for Olefin Homo- and Copolymerization: Relationships between Catalyst Structures and Catalytic Properties. *Chem. Rev.* **2015**, *115*, 12091−12137.

(24) Wang, Z.; Liu, Q.; Solan, G. A.; Sun, W.-H. Recent advances in Ni-mediated ethylene chain growth: N_{imine}-donor ligand effects on catalytic activity, thermal stability and oligo−/polymer structure. *Coord. Chem. Rev.* **2017**, *350*, 68−83.

(25) Younkin, T. R.; Connor, E. F.; Henderson, J. I.; Friedrich, S. K.; Grubbs, R. H.; Bansleben, D. A. Neutral, Single Component Nickel (II) Polyolefin Catalysts That Tolerate Heteroatoms. *Science* **2000**, *287*, 460−462.

(26) Chen, Z.; Leatherman, M. D.; Daugulis, O.; Brookhart, M. Nickel-Catalyzed Copolymerization of Ethylene and Vinyltrialkoxysilanes: Catalytic Production of Cross-Linkable Polyethylene and Elucidation of the Chain-Growth Mechanism. *J. Am. Chem. Soc.* **2017**, *139*, 16013−16022.

(27) Chen, Z.; Brookhart, M. Exploring Ethylene/Polar Vinyl Monomer Copolymerizations Using Ni and Pd α-Diimine Catalysts. *Acc. Chem. Res.* **2018**, *51*, 1831−1839.
(28) Liang, T.; Chen, C. Position Makes the Difference: Electronic Effects in Nickel-Catalyzed Ethylene Polymerizations and Copolymerizations. *Inorg. Chem.* **2018**, *57*, 14913−14919.
(29) Hong, C.; Sui, X.; Li, Z.; Pang, W.; Chen, M. Phosphine phosphonic amide nickel catalyzed ethylene polymerization and copolymerization with polar monomers. *Dalton Trans.* **2018**, *47*, 8264−8267.
(30) Tao, W. J.; Nakano, R.; Ito, S.; Nozaki, K. Copolymerization of Ethylene and Polar Monomers by Using Ni/IzQO Catalysts. *Angew. Chem., Int. Ed.* **2016**, *55*, 2835−2839.
(31) Xin, B. S.; Sato, N.; Tanna, A.; Oishi, Y.; Konishi, Y.; Shimizu, F. Nickel Catalyzed Copolymerization of Ethylene and Alkyl Acrylates. *J. Am. Chem. Soc.* **2017**, *139*, 3611−3614.
(32) Zhang, Y.; Mu, H.; Pan, L.; Wang, X.; Li, Y. Robust Bulky [P,O] Neutral Nickel Catalysts for Copolymerization of Ethylene with Polar Vinyl Monomers. *ACS Catal.* **2018**, *8*, 5963−5976.
(33) Chen, M.; Chen, C. A Versatile Ligand Platform for Palladium- and Nickel-Catalyzed Ethylene Copolymerization with Polar Monomers. *Angew. Chem., Int. Ed.* **2018**, *57*, 3094−3098.
(34) Laine, T. V.; Piironen, U.; Lappalainen, K.; Klinga, M.; Aitola, E.; Leskelä, M. Pyridinylimine-based nickel(II) and palladium(II) complexes: preparation, structural characterization and use as alkene polymerization catalysts. *J. Organomet. Chem.* **2000**, *606*, 112−124.
(35) Sun, W.-H.; Song, S.; Li, B.; Redshaw, C.; Hao, X.; Li, Y.-S.; Wang, F. Ethylene polymerization by 2-iminopyridylnickel halide complexes: synthesis, characterization and catalytic influence of the benzhydryl group. *Dalton Trans.* **2012**, *41*, 11999−12010.
(36) Irrgang, T.; Keller, S.; Maisel, H.; Kretschmer, W.; Kempe, R. Sterically Demanding Iminopyridine Ligands. *Eur. J. Inorg. Chem.* **2007**, 4221−4228.
(37) Chen, Z.; Allen, K. E.; White, P. S.; Daugulis, O.; Brookhart, M. Synthesis of Branched Polyethylene with "Half-Sandwich" Pyridine-Imine Nickel Complexes. *Organometallics* **2016**, *35*, 1756−1760.
(38) Antonov, A. A.; Semikolenova, N. V.; Talsi, E. P.; Matsko, M. A.; Zakharov, V. A.; Bryliakov, K. P. 2-iminopyridine nickel(II) complexes bearing electron-withdrawing groups in the ligand core: Synthesis, characterization, ethylene oligo- and polymerization behavior. *J. Organomet. Chem.* **2016**, *822*, 241−249.
(39) D'Auria, I.; Milione, S.; Caruso, T.; Balducci, G.; Pellecchia, C. Synthesis of hyperbranched low molecular weight polyethylene oils by an iminopyridine nickel(II) catalyst. *Polym. Chem.* **2017**, *8*, 6443−6454.
(40) Dai, Q.; Jia, X.; Yang, F.; Bai, C.; Hu, Y.; Zhang, X. Iminopyridine-Based Cobalt(II) and Nickel(II) Complexes: Synthesis, Characterization, and Their Catalytic Behaviors for 1,3-Butadiene Polymerization. *Polymer* **2016**, *8*, 12.
(41) Figueira, C. A.; Lopes, P. S.; Gomes, C. S.; Gomes, J. C. S.; Veiros, L. F.; Lemos, F.; Gomes, P. T. Neutral Mono(5-aryl-2-iminopyrrolyl)nickel(II) Complexes as Precatalysts for the Synthesis of Highly Branched Ethylene Oligomers: Preparation, Molecular Characterization, and Catalytic Studies. *Organometallics* **2019**, *38*, 614−625.
(42) Dall'Anese, A.; Rosar, V.; Cusin, L.; Montini, T.; Balducci, G.; D'Auria, I.; Pellecchia, C.; Fornasiero, P.; Felluga, F.; Milani, B. Palladium-Catalyzed Ethylene/Methyl Acrylate Copolymerization: Moving from the Acenaphthene to the Phenanthrene Skeleton of α-Diimine Ligands. *Organometallics* **2019**, *38*, 3498−3511.
(43) Mancin, F.; Tecilla, P.; Tonellato, U. Metallomicelles Made of Ni(II) and Zn(II) Complexes of 2-Pyridinealdoxime-Based Ligands as Catalyst of the Cleavage of Carboxylic Acid Esters. *Langmuir* **2000**, *16*, 227−233.
(44) Zhang, Y.; Wang, C.; Mecking, S.; Jian, Z. Ultrahigh Branching of Main-Chain-Functionalized Polyethylenes by Inverted Insertion Selectivity. *Angew. Chem., Int. Ed.* **2020**, *59*, 14296−14302.
(45) Ray, S.; Rao, P. V. C.; Choudary, N. V. Poly-α-olefin-based synthetic lubricants: a short review on various synthetic routes. *Lubr. Sci.* **2012**, *24*, 23−44.

https://dx.doi.org/10.1021/acs.macromol.0c01703
Macromolecules 2020, 53, 9294−9305